Magnetic-Field-Induced Metal-Insulator Transitions in Multiple-Quantum-Well Structures

Y. J. Wang and B. D. McCombe
Department of Physics, State University of New York at Buffalo, Buffalo, New York 14260

R. Meisels and F. Kuchar
Institut für Physik, Montanuniversität Loeben, A-8700 Loeben, Austria

W. Schaff
School of Electrical Engineering, Cornell University, Ithaca, New York 14853
(Received 20 May 1993)

Far infrared spectroscopy and electrical transport measurements on a set of modulation-doped GaAs/$Al_{0.3}Ga_{0.7}As$ multiple-quantum-well structures show metallic and insulating behavior that depends on doping density and magnetic field; impurity band insulator, impurity band metal, and quantum Hall conductor states are observed. In the latter case a plateau around filling factor 1 shows entrance to an insulating state at higher fields; this result is compared with the global phase diagram for the quantum Hall effect. A general phase diagram that encompasses lower doping densities is suggested.

PACS numbers: 71.30.+h, 72.20.My, 73.20.Dx, 78.65.–s

Numerous interesting electronic phenomena occur at high magnetic fields in high quality quasi-two-dimensional (Q2D) electron gas systems at low temperature, e.g., the integer quantum Hall effect (IQHE), the fractional quantum Hall effect (FQHE), and Wigner crystallization. Disorder and electron localization are intimately connected to these phenomena. Recently, Kivelson, Lee, and Zhang have proposed a global phase diagram (GPD) [1] for the quantum Hall effect in a plot of disorder versus magnetic field, including predicted transitions from the quantum Hall conductor state to different insulating states at high magnetic fields. The various conducting and insulating states in Q2D systems and the transitions between such states and their dependences on magnetic field and other parameters are of fundamental interest.

Considerable work on the metal-insulator transition (MIT) has been carried out on doped bulk semiconductors [2–7] and in certain Q2D systems [8–10]. For such studies modulation-doped quantum-well (QW) structures posses a number of advantages compared with either bulk semiconductors or single heterostructures. In addition to control of wave function overlap provided by magnetic field and dopant density (average impurity separation), in QWs the electron wave function extent in the well(s) can be controlled by the well-width and the set-off distance of the shallow donors in the barriers while maintaining the confining potential essentially unchanged. In such structures electrons from donor impurities located in the barriers are transferred to the well(s), and at low doping densities are weakly bound to their parent donors in the barriers [with wave functions localized in the well(s)] in well-defined, discrete energy states that are well understood [11]. In order to provide adequate absorption strength to observe the impurity transitions spectroscopically at low doping densities, multiple QW structures are usually required. At higher densities impurity bands are formed [12], and at sufficiently high doping densities and sufficiently low disorder the IQHE and FQHE occur at high fields. Systematic studies of the magnetic-field-induced MITs in this model Q2D system can provide useful insight into the connections between the quantum Hall conductor and various insulating states, and also into the evolution and development of the quantum Hall conductor itself from the insulating and metallic states that occur at lower doping densities. These transitions, particularly in the low-density region, have not been previously explored.

We report far infrared optical and electrical transport studies of a series of modulation-doped GaAs/AlGaAs MQW samples over regions of magnetic field and shallow donor doping densities in the barriers that encompass various metallic and insulating states. Far infrared magnetotransmission measurements were carried out at temperatures between 1.5 and 30 K in magnetic fields up to 9 T with a Fourier transform spectrometer, light-pipe-condensing-cone optics, and both photoconductive (Ge:Ga) and bolometric (doped Si) detectors. Electrical transport measurements were made at temperatures between 0.3 and 15 K in magnetic fields up to 11 T by conventional dc and low frequency ac techniques. Results on three molecular beam epitaxy (MBE) grown, modulation-doped (over the central $\frac{1}{3}$ of the $Al_{0.3}Ga_{0.7}As$ barriers with Si donors) MQW structures (24 nm by 24 nm) are described; barrier doping densities are 3.2×10^{10} cm^{-2} (sample 1), 8×10^{10} cm^{-2} (sample 2), and 1.5×10^{11} cm^{-2} (sample 3). These data show transitions from impurity-band metal to impurity-band insulator at low doping densities, and, at higher doping densities, a transition to a quantum Hall conductor state, which enters an insulating state at magnetic fields above the quantum Hall plateau at integer filling factor $\nu = 1$.

 0031-9007/95/75(5)/906(4)$06.00

Results of the magnetotransmission measurements are summarized in Fig. 1, in which the frequency of the dominant transmission minimum for each sample at 4.2 K is plotted versus magnetic field. For sample 1 the experimental results are in good agreement with variational calculations for the ground state $m = 0$ to the first excited state with $m = +1$ (m is the quantum number for projection of orbital angular momentum along B) for *isolated impurities* located at the barrier centers [11]; at higher temperatures a distinct, sharp cyclotron resonance (CR) absorption line was observed whose amplitude increased with temperature at the expense of the impurity line. For sample 2 the observed transitions are also in good agreement with the isolated impurity calculations at fields above 5 T, but the measured values at lower fields deviate to higher frequencies. In the low field region the impurity lines for this sample are substantially broader than those of sample 1.

The diagonal and Hall resistances (R_{xx} and R_{xy}) of sample 1 showed activated behavior over the entire range of fields and temperatures investigated. However, as shown in Fig. 2(a), sample 2 behaves very differently. Below 3 T the sheet density N_d obtained from the Hall voltage is approximately independent of temperature (metallic behavior) and increases slightly with magnetic field [13]. Above 3 T the electron density is thermally activated with a (small) activation energy that increases with magnetic field.

The two main types of MITs that are observable at He temperatures in semiconductors are the Mott transition and the Anderson transition. (We do not consider weak localization.) In the simplest picture the Mott MIT takes place in a semiconductor with a periodic impurity sublattice when, due to overlap of the electronic wave functions, the upper Hubbard (UH) band, which evolves from the discrete negative donor ion ground state (two electrons on a single impurity site), merges with the lower Hubbard (LH) band, the one-electron impurity band that evolves from the discrete neutral donor ground state [14].

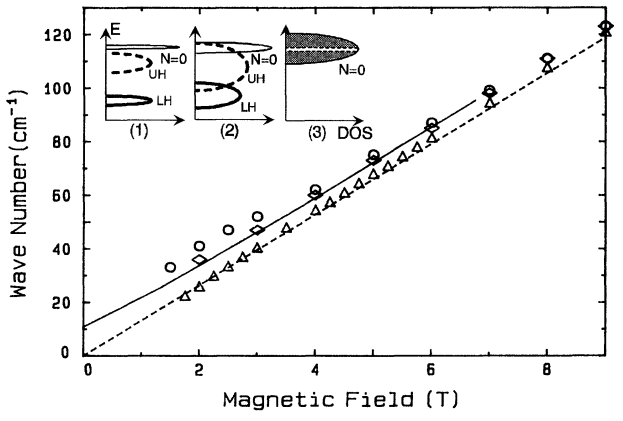

FIG. 1. Magnetotransmission minima vs magnetic field at 4.2 K: ◇, sample 1; ○, sample 2; and △, sample 3. Dashed line: CR; solid line: calculated transition energy for isolated, barrier-center donors [11]. Inset: Schematic diagrams of the density of states associated with the lowest Landau level for samples (1)–(3) at low magnetic fields. The hatched region in (3) indicates localized states. There are similar, small regions (not shown) in the UH and LH bands.

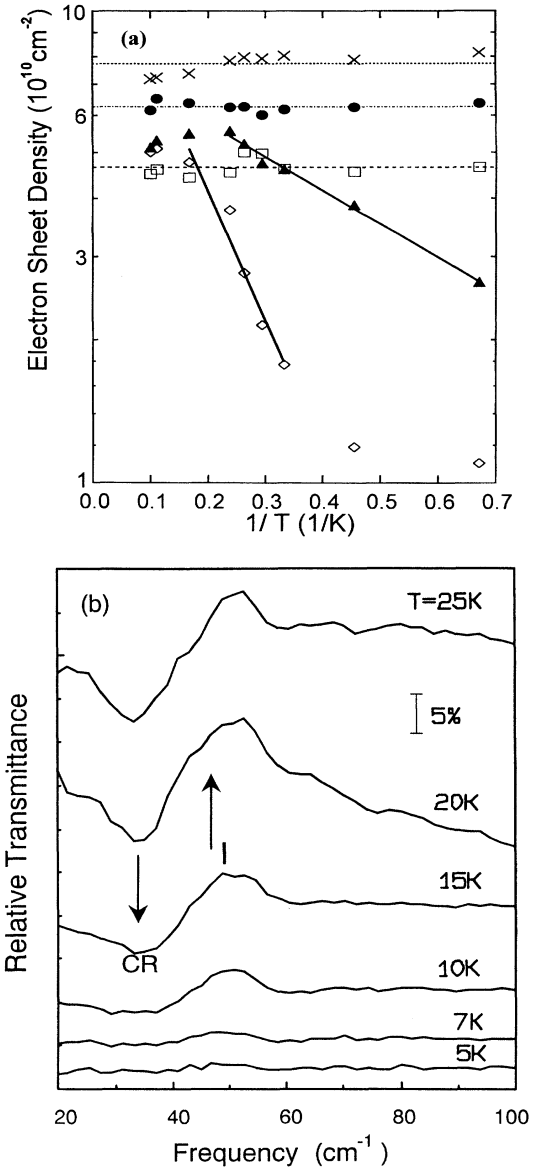

FIG. 2. (a) Semilogarithmic plot of electron sheet density ($\propto 1/R_{xy}$) of sample 2 as a function of $1/T$ at several magnetic fields: □, 0.5 T; ●, 1.5 T; ×, 2.5 T; ▲, 4.0 T; and ◇, 6.0 T. Data for 2.5 and 1.5 T have been shifted up by 50% and 30%, respectively, for clarity. Solid lines are exponential fits to the data at 4 and 6 T with activation energies of 1.6 and 7.8 K, respectively. The deviation of the data points at 6 T and about 2.5 K is due to the onset of variable range hopping within the lowest impurity band. (b) Temperature dependence of relative transmission (transmitted intensity at the indicated temperature divided by the transmitted intensity at 4.2 K) of sample 2 in the region of metallic electrical conductivity (2.5 T). Arrows show the positions of CR and the impurity transition observed at 4.2 K (I).

The mechanism that gives rise to a MIT in this case is electron-electron Coulomb repulsion. The Anderson transition, in contrast, occurs in a disordered one-electron system with random potential fluctuations in the absence of electron-electron interactions; the electronic states are all localized for sufficiently strong disorder. In experimentally realizable structures, some combinations of the two mechanisms is responsible for the observed MITs.

An approximate criterion for the Mott transition (insulator to metal) in the present Q2D situation is $(N_{2D})^{1/2}a_B = M \geq 0.3$ at zero magnetic field [15], where a_B is the effective Bohr radius. For the present samples a_B for center-barrier impurities is $\approx$17 nm [15]. $M \approx 0.3$ for sample 1 and 0.48 for sample 2; therefore ideally at zero magnetic field sample 1 should be on the borderline, and sample 2 should be metallic. Because of topological disorder, compensation, and well-width fluctuations, there will be some localized states near the edges of the UH and LH bands which will favor the insulating state. An applied magnetic field normal to the sample surface shrinks the electron wave function in the plane; for such a large Bohr radius the magnetic field can have a substantial effect on the impurity wave functions and their overlap.

With this preamble it is clear that the results for these samples qualitatively fit a modified Mott picture. Sample 1 should be insulating due to residual disorder at zero magnetic field; a magnetic field reduces wave function overlap, narrows the LH and UH bands, and increases any energy separation between extended states in these bands. A schematic density of states (DOS) picture for this situation is shown as (1) in the inset to Fig. 1. If insulating at zero field, the sample should remain insulating at all magnetic fields and should have well-defined neutral donor impurity ground- and excited-state bands (LH bands), as observed. With low disorder, sample 2 ($M = 0.48$) should show metallic electrical properties at low magnetic fields [sketch (2) in the inset to Fig. 1]. Above about 3 T the reduced bandwidth due to wave function shrinkage causes a gap to open up between extended states in the LH and UH bands; thus the sample becomes insulating with a small electrical activation energy that increases with magnetic field. As discussed below, in the region where *metallic* behavior is clearly observed in the transport measurements, the magnetotransmission spectra show definite *impurity-related* lines, not free carrier CR; thus the chemical potential is still located in a well-defined impurity band having a peak in its DOS below the lowest Landau level, not in extended states *in* the Landau level. In this sense the MIT takes place within the impurity band.

The LH bands for sample 2 are well defined even in the region of metallic dc conductivity, as demonstrated in Fig. 2(b), which shows the temperature dependence of transmission spectra at 2.5 T. The data are ratioed to show clearly the evolution from impuritylike (LH band) transitions at low temperature to free carrier CR at higher temperatures. The ratio of a spectrum with CR dominant to a spectrum with impurity-band transition dominant will give rise to a *dip* at low frequency and a *peak* at high frequency. Above 10 K the ratios show this behavior. When temperature is raised, the free carrier CR signal (at 33 cm^{-1}) gradually increases in strength due to thermal excitation into extended Landau level states, replacing the impurity band transition (at $\sim$50 cm^{-1}), which is dominant at low temperatures. The activation energy for this process is characteristic of the energy difference between the top of the LH band and the Landau level. The observed position of the dip is exactly at the position of CR at 2.5 T (arrow), and the position of the peak occurs close to the position of the impurity transition measured at low temperatures. Thus the magneto-optical transitions retain strong impurity character, while the transport results show clear metallic behavior, consistent with a Mott picture modified to account for the magnetic field.

Sample 3 ($N_d = 1.5 \times 10^{11}$ cm^{-2}) shows very different electrical transport and magnetotransmission behavior. As shown in Fig. 3, there are clear plateaus in R_{xy} and minima in R_{xx} at 0.35 K at fields corresponding to $\nu = 1$, 2, and 4. At fields higher than $\nu = 1$, both R_{xy} and R_{xx} increase very rapidly with increasing magnetic field. At about 10 T ($\nu = \frac{1}{2}$), $R_{xx} = 5$ MΩ, 20 times R_{xx} at $B = 0$, and $R_{xy} = 10$ kΩ, which is larger than the value of R_{xy} corresponding to $\nu = \frac{1}{3}$ (7.8 kΩ—10 layers of this sample are electrically contacted) at about 15 T. Both R_{xx} and R_{xy} increase very strongly for $\nu < 1$ when temperature is lowered from 4.2 to 0.35 K, which suggests that both approach infinity as $T \rightarrow 0$ in this region; the sample is in some type of insulating state [16], consistent with the global phase diagram for the IQHE [1]. For sufficient disorder the FQHE is suppressed (the mobility of this sample is only about 30 000 $cm^2/V\,s$), and the sample becomes an insulator after completion of the last integer plateau. One possible insulating phase in this region is the so-called Hall insulator, which has the unique property that R_{xx} goes to infinity, but R_{xy} follows roughly the classical value B/nec as B is increased beyond the

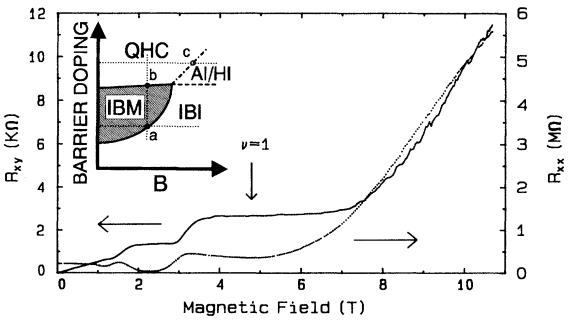

FIG. 3. Plot of R_{xx} (dashed line) and R_{xy} (solid line) for sample 3 at 0.35 K vs magnetic field. Inset: Schematic phase diagram for a modulation-doped MQW system with weak disorder: AI, Anderson insulator; HI, Hall insulator; IBM, impurity-band metal; IBI, impurity-band insulator; QHC, quantum Hall conductor.

last plateau. The Hall insulator is favored if the shortest length scale in the system is the magnetic length l_B, rather than the elastic mean free path l_e [1]. For this sample $l_B = 11.3$ nm at 5 T and l_e is estimated from the low field mobility and carrier density to be approximately 100 nm; thus the Hall insulator is favored [17]. From Fig. 3 it is clear that R_{xy} *does not* follow the classical value. In spite of the apparent divergent behavior of R_{xy} it is still possible that the sample is a Hall insulator but in a region of parameter space where R_{xy} is weakly diverging [1].

In contrast to sample 2, magnetotransmission measurements on sample 3 show *sharp* lines with transmission minima close to the frequencies expected for CR at this well-width (Fig. 1). At low fields the measured minima fall on the CR line of Fig. 1 within experimental error; however, above 4–5 T the observed frequencies are shifted 1–2 cm^{-1} above the CR line. The observed shift takes place gradually in the vicinity of $\nu = 1$. In this quantum limit the observed transitions at high fields are shifted up in frequency compared to CR because, as field is increased beyond $\nu = 1$, a larger and larger fraction of the electrons are localized in the valleys of the long range lateral potential fluctuations caused primarily by the smoothed out (due to the fact that the average separation of the impurities is approximately equal to the separation between the doping sheet and the electrons in the wells) and self-consistently screened potential of the positive impurity ions in the barriers. The weak lateral confinement due to the potential fluctuations gives rise to a shifted CR [18]. At these high densities electrons do not "see" individual positive ions with identical Coulomb potential, but rather move in a weak, long range (compared to the CR orbit size l_B), random potential; the potential fluctuations as "measured" by this shift must clearly be longer range than the magnetic length. Therefore electrons in this sample in high magnetic fields no longer see the discrete impurity potentials, nor is there any observable remainder of the well-defined (by the peak in the DOS) impurity band that provides a good description of the situation at lower barrier doping densities. The electron system is now more appropriately described by the Anderson model with electron-electron correlations. [The DOS at low fields is sketched in (3) of the inset to Fig. 1]. The transition between the impurity band (Mott) picture and the Anderson model takes place when the average lateral separation between impurities in the barrier becomes approximately equal to or less than the distance between the electrons and the doping sheet in the barrier (~24 nm for the present samples).

Results are summarized by the schematic phase diagram in the inset to Fig. 3. At a fixed low magnetic field (vertical cut), as the doping density is increased, there is a transition at point (a) from an impurity-band insulator (sample 1) to an impurity-band metal (sample 2), and finally at point (b) to a quantum Hall conductor (sample 3). At moderate fixed values of barrier doping density, as the magnetic field is increased (lower horizontal cut), the system is initially an impurity-band metal and undergoes a transition at point (a) to an impurity-band insulator (sample 2). At sufficiently high barrier doping density (upper horizontal cut) at small values of magnetic field the electrons form a quantum Hall conductor (the weak localization insulator at $B = 0$ [19], which was not observed in our measurements, is not shown), which at high enough magnetic fields becomes either an Anderson insulator (AI) or a Hall insulator (HI) at point (c) (sample 3). The region covered by the GPD [1] lies above the (nearly) horizontal solid and dashed lines in the upper part of the inset.

We are grateful to Y. C. Lee and D. H. Lee for useful discussions and to L. P. Fu, W. C. Chou, and A. Petrou for optical characterization. This work was supported in part by NSF Grant No. INT-86-19783 and ONR Grant No. N000-14-89-J-167.

[1] S. Kivelson, D.-H. Lee, and S.-C. Zhang, Phys. Rev. Lett. **46**, 2223 (1992).
[2] D. Romero, S. Liu, H. D. Drew, and K. Ploog, Phys. Rev. B **42**, 3179 (1990).
[3] G. A. Thomas, M. Burns, P. Hopkins, and R. M. Westervelt, Philos. Mag. **56**, 687 (1987).
[4] M. W. Lee, D. Romero, H. D. Drew, M. Shaygan, and B. S. Elman, Solid State Commun. **66**, 23 (1988).
[5] J. Stankiewicz, S. von Molnar, and W. Giriat, Phys. Rev. B **33**, 3573 (1986).
[6] Peihua Dai, Youzhu Zhang, and M. Sarachik, Phys. Rev. B **46**, 6724 (1992).
[7] R. F. Milligan and G. A. Thomas, Annu. Rev. Phys. Chem. **36**, 139 (1985).
[8] J. L. Robert, A. Raymond, L. Koncewicz, C. Bousquet, W. Zawadzki, F. Alexandre, I. M. Masson, J. P. Andre, and P. M. Frijlink, Phys. Rev. B **33**, 5935 (1986).
[9] H. Sigg, K. von Klitzing, M. Hauser, and K. Ploog, in *Shallow Impurities in Semiconductors,* edited by B. Monemar (Institute of Physics, Bristol, 1988), p. 11.
[10] See, e.g., T. Ando, A. B. Fowler, and F. Stern, Rev. Mod. Phys. **54**, 437 (1982).
[11] Experimental, A. A. Reeder *et al.,* IEEE J. Quantum Electron **24**, 1690 (1988); theoretical, R. L. Greene, and P. Lane, Phys. Rev. B **34**, 8639 (1986).
[12] See, e.g., J. Serre, A. Ghazali, and A. Gold, Phys. Rev. B **39**, 8499 (1989).
[13] M. Shayegan, V. J. Goldman, and H. D. Drew, Phys. Rev. B **38**, 5585 (1988).
[14] See, e.g., N. F. Mott, *Metal-Insulator Transitions* (Taylor and Francis, London, 1974).
[15] Y. J. Wang, Ph.D. thesis, SUNY at Buffalo, 1993 (unpublished).
[16] Early work on single heterostructures showed similar behavior: M. A. Paalanen, D. C. Tsui, B. J. Lin, and A. C. Gossard, Surf. Sci. **142**, 29 (1984).
[17] Since R_{xx} is so large, even a 0.1% admixture could mask Hall insulator behavior in R_{xy}.
[18] J. Richter, H. Sigg, K. v. Klitzing, and K. Ploog, Phys. Rev. B **39**, 6268 (1989); J.-P. Cheng and B. D. McCombe, Phys. Rev. Lett. **64**, 3171 (1990).
[19] See, e.g., H. W. Jiang, C. E. Johnson, K. L. Wang, and S. T. Hannahs, Phys. Rev. Lett. **71**, 439 (1993).